STUDY ON TEMPERATURE FIELD OF ASYMMETRIC LARGE-SPAN ARCH SHEDS UNDER LOW-TEMPERATURE ENVIRONMENT
/
非对称大跨度拱棚低温环境下的温度场研究

Kai Zhou[1)], Zhiwei Meng[1)], Min Wei[2)], Jialin Hou[1)], Tianguo Jin[3)], Tianhua Li*[1)]
[1)] College of Mechanical and Electronic Engineering, Shandong Agricultural University, Taian 271018, China;
[2)] College of Horticulture Science and Engineering, Shandong Agricultural University, Taian 271018, China;
[3)] School of Mechatronics Engineering, Harbin Institute of Technology, Harbin 150001, China.
Tel: 18853876906; E-mail: litianhua689@163.com
DOI: https://doi.org/10.35633/inmateh-62-25

Keywords: *asymmetric structure, large-span arch shed, numerical simulations, response surface methodology*

ABSTRACT

In order to improve the effective sunshine time, heat storage capacity and temperature distribution uniformity of traditional arch shed under low temperature, this paper designed a large-span arch shed which has larger sunny side span and east-west orientation. According to the numerical and measured data, it is concluded that the heat storage capacity and temperature distribution of asymmetrical arch shed are better than those of symmetrical arch shed within a certain range of the ratio between sunny and shaded side. After that, ten different asymmetric arch sheds were designed. It is concluded that the structure of 11+9 m along north-south direction has the best heat storage capacity. Besides that, the analysis of outside wind speed and opening size of top vent were carried out. It is found that the outside wind and top vent can effectively promote convection and exchange of the air, and then achieve the purpose of reducing the temperature. At the end of this paper, in order to identify the relationship of temperature with the structure of arch shed, outside wind speed, and opening size of top vent, a mathematical model was built based on response surface methodology, which would provide theoretical guidance for the design of arch sheds.

摘要

为提升传统拱棚低温环境下的有效日照时间、蓄热能力和温度分布均匀性，该文设计了一种东西走向的非对称大跨度拱棚。由数值计算和实测数据可以得出，向阳面和背阴面的跨度比在一定范围内时，非对称拱棚的蓄热能力和温度分布均匀性要优于对称拱棚。在此基础上，设计了 10 种不同的非对称拱棚，结果表明沿南北方向的 11+9 m 拱棚的蓄热能力最优。此外，对外界风速和顶通风口开度进行分析，研究发现外界风速和顶通风口能够能有效促进棚内空气对流和交换，进而降低棚内温度。最后，为了确定温度与拱棚结构、外界风速和顶部通风口开度之间的关系，基于响应曲面法建立了数值模型，为拱棚设计提供了理论指导。

INTRODUCTION

Arch shed is a type of greenhouse generally used in facility agriculture *(Changji Zhou and Yingkuan Wang, 2001)*. Compared with solar greenhouse, arch shed without heat-storage wall has the advantage of high space utilization rate, simple construction, and good durability, but the performances of heat storage and thermal insulation are usually poor *(Fei Qi et al., 2008; López-Martínez J. et al., 2018; Saberian A. and Sajadiye S.M., 2019)*. Besides that, the arch sheds usually have relatively smaller span to enhance the thermal insulation. With the in-depth studies on the performance of arch sheds, it is found that expanding the space of arch shed could not only enhance the cushioning performance against external environment, increase the space utilization rate, but also facilitate the mechanization operations. In addition, arch shed with large span could improve the heat storage capacity and illuminating uniformity significantly, and the thermal insulation at night is ensured by insulation coverage, so the large-span arch sheds have got rapid developments *(Xiangli He et al., 2017; Bartzanas T. et al., 2004; Kim K. et al., 2008)*. Especially in recent years, the east-west asymmetric arch shed has begun to appear in production, which has a larger sunny side to increase illumination area *(Mobtaker H.G. et al., 2016)*.

In the past, the researches on arch sheds mostly focused on the north-south symmetric arch shed. Furthermore, the researches mainly studied the influences of ventilation mode and outside environment to the flow field and temperature field in the arch shed *(Majdoubi H. et al., 2009)*. For the east-west asymmetric arch shed, the influence of geometric structure to performance is an important research content. Similarly, the ventilation mode and the outside environment also have important impacts on performance of the arch shed.

However, there are few related studies in this area *(Singh R.I. et al., 2013; Guohui Gan, 2009; Perén J.I. et al., 2015)*.

With the developments of CFD (computational fluid dynamics) and computer technology, CFD has been widely applied in the field of greenhouse. CFD method can obtain the detailed information of flow field and thermal environment, the cost is lower, and the repeatability is better, which has a great advantage in revealing the air flow behaviour and heat transfer in the arch shed. However, numerical simulations based on CFD generally need to combine the test method to set the boundary conditions and calculation parameters. Besides that, the reliability of numerical results should be verified by test results *(Guohong Tong et al., 2018; Ghenai C. and Janajreh I., 2010; Kruggel-Emden H. et al., 2010)*.

The paper combined numerical method and experimental method, and analyses aiming at the east-west large-span asymmetric arch shed were conducted, which attempted to explore the mechanism of air flow behaviour and heat transfer in the arch shed, analyse the influence factors, and then enhance the performance of the arch shed. Finally, the response surface methodology was adopted to identify the relationship of temperature with structure of arch shed, outside wind speed, and opening size of top vent, which would provide theoretical guidance for the design and construction of arch sheds in different regions and for different needs.

MATERIALS AND METHODS

- **Geometric modelling**

Based on relevant studies and industry standards, the east-west length of the arch shed is set as 50 m, the north-south span is set as 20 m, and the height of the arch shed is set as 6.5 m. The arch shed is equipped with top vent and side vent to realize ventilation. For example, the detailed structural parameters of 13+7 m arch shed are shown in Figure 1. The other structural parameters can be obtained by scaling proportionally.

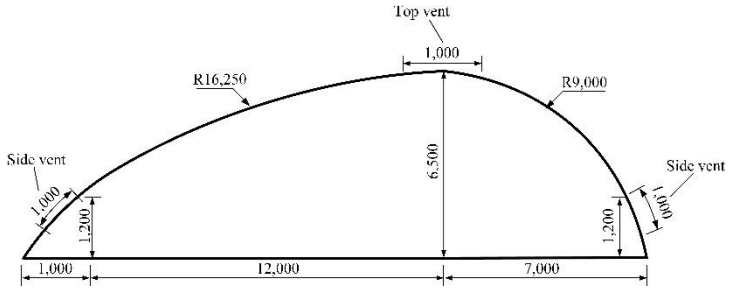

Fig. 1 - Geometric parameter of the arch shed

- **Test arch shed and measuring method**

Taking into account the construction cost, two east-west asymmetric arch sheds with a north-south sunny side span of 15 m and 13 m were constructed (North latitude 36°14', East longitude 117°32'), and a symmetric arch shed was constructed as a comparison, which is shown in Figure 2. From November 2018 to April 2019, temperature and outside wind speed were collected by sensors to exploring the differences among the three arch sheds. The test period has typical characteristics of temperate monsoon climate in the northern hemisphere, which can be described as cold, dry, and calm *(Guzmán C. et al., 2019)*.

a) *b)* *c)*

Fig. 2 - Test arch sheds

a) 13+7 m arch shed; *b)* 15+5 m arch shed; *c)* 10+10 m arch shed

The temperature sensors are arranged as shown in Figure 3. The acquisition frequency is half an hour, and the data is summarized once a month. After the on-the-spot investigation, the heat preservation quilt was covered daily from 16:00 to 8:00 during the test period, and the top vents were opened daily from 12:00 to 14:00 while the side vents remained closed. The outside wind speed and direction was measured by automatic recorder, which was placed 1.5 m height in front of the arch shed. There were no crops in the arch sheds during the test period.

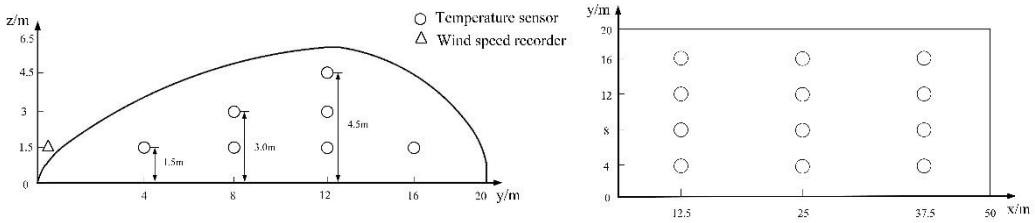

a) *b)*

Fig. 3 - Sensors arrangement

a) Vertical distribution of sensors *b) Horizontal distribution of sensors*

- **Numerical modelling and solving**

Mesh generation

In order to ensure the accuracy of numerical simulations, the air field outside the arch shed is conducted as a part of computational domain. And the dimension of computational domain is twice as large as the arch shed, which could fully consider the convection effect between the inside and outside air field. The arch shed is placed in the centre of calculation domain, with x-axis direction as the east direction and y-axis direction as the north direction.

Tetrahedral elements are used, and the fluid domain is divided into about 2×10^6 grid cells. Besides, refined mesh is adopted near the vents. To verify the grid independency, the simulation with smaller cell size is carried out and only 4% of the difference between the coarse grid and the fine grid is found. It can be concluded that, when the number of grid divisions is larger than 2×10^6, the numerical results are independent of grid divisions, and the scheme of grid division is reasonable.

Boundary condition and solving method

The physical characteristic parameters of air, soil and shed plastic film are shown in Table 1. The east boundary of the outside fluid domain is set as velocity-inlet boundary, the west boundary is set as pressure-outlet boundary, the ground and shed film are set as wall boundary, and the other boundaries are set as symmetry boundary, which is shown in Figure 4. The temperature of ground and outside air field are set according to the measured data. The shed film is set to PE (polyethylene) material with a thickness of 0.1 mm. The radiation transmission type is set to semi-transparent material. In addition, the radiation absorptivity of shed film is set to 0.28, and the radiation transmissivity is set to 0.7. In order to fully consider the influences of radiation and air convection to the thermal environment, the DO (discrete ordinate) solar model is used. And the heat exchange is solved by coupling method between inside and outside of the plastic film. Moreover, the standard k-ε model is chosen as turbulence model, the second-order upwind scheme is adopted to discrete calculation, and the SIMPLE algorithm is used for steady-state solving *(Piscia D. et al., 2012; Banu J.P. and Mani A., 2019; Kichah A. et al., 2012)*.

Thermal physical properties of materials **Table 1**

Material	Density/(kg·m^{-3})	Specific heat/(J·kg^{-1}·K^{-1})	Thermal conductivity/(W·m·K^{-1})
Soil	1,200	2,500	1.5
PE	923	2,200	0.34
Air	1.18	1.003	1.003

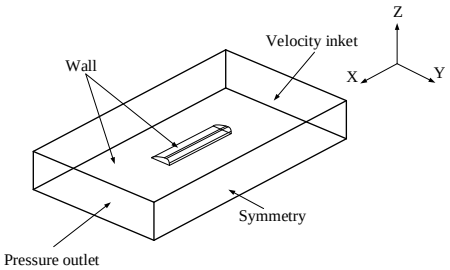

Fig. 4 - Boundary conditions

RESULTS AND ANALYSIS

- **Analysis of temperature field**

Analysis of measured data

All crops have requirements for suitable temperature for growth. Take tomatoes for example, the temperature should be kept within the range of 25°C to 28°C in the daytime and 13°C to 15°C at night.

The arch shed should have the capacity of heat storage and insulation to guarantee the growth of vegetables, especially under low temperature in the winter. The measured temperatures in 13+7 m arch shed on January 6th are shown in the figure below. The weather was fine that day, and the wind speed was about 0.3 m/s. The opening size of top vent was 0.3 m from 12:00 to 14:00.

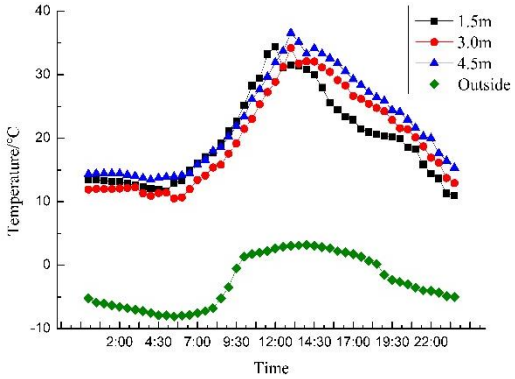

Fig. 5 - Temperature of 13+7 m arch shed over the day

It can be seen that the average temperature curves at different heights have the similar trends, and the inside temperature is obviously higher than outside temperature. According to the measured data in other north-south arch sheds, the average temperature in the daytime of east-west arch shed is significantly higher. Specifically, the temperature at the height of 1.5 m in the arch shed is 13.53°C at 0:00, and drops to 11.71°C at 5:00. This is because there is no solar radiation for a long time, and the heat is gradually transferred from inside to outside. From 7:00 to 12:00, the temperature in the shed rises fast with the decrease of solar angle of incidence. Moreover, the temperature increases in the arch shed with the increasing of the height. From 12:00 to 14:00, the temperature dropped gradually because of the opening of top vent resulting in air convection between inside and outside. After 14:00, as solar angle of incidence gradually increases, the temperature in the arch shed begins to decrease, and the heat is gradually transferred from inside to outside. Based on relevant studies, numerical simulations in the following analysis are conducted at 14:00, which can obviously reflect the heat storage capacity of the arch shed.

Table 2 shows the comparison of the average temperature at each height between the symmetrical and asymmetrical arch sheds. It can be found that the temperature in the three arch sheds gradually decreased from top to bottom, with the lowest temperature near the ground. This is because the hotter air accumulates in the upper layer to raise the temperature, and the ground with large specific heat capacity absorbs heat from the air, so the temperature near the ground is lowest. Compared with the 10+10 m arch shed, the average temperature of 13+7 m arch shed is increased by 2.97%, 3.95% and 5.62% respectively at the three heights. However, the temperature of 15+5 m arch shed is relatively lower. It is concluded that the heat storage capacity of asymmetrical arch shed is better than that of symmetrical arch shed within a certain range of the ratio between the sunny side and the shaded side.

Vertical distribution of temperature **Table 2**

Arch shed structure	1.5 m/°C	3 m/°C	4.5 m/°C
10+10 m	29.96	30.89	31.52
13+7 m	30.85	32.11	33.29
15+5 m	28.41	29.06	30.58

According to Figure 3, the measured data of the three arch sheds are divided into three groups of east, middle and west. The data are shown in Table 3.

East-west distribution of temperature **Table 3**

Arch shed structure	Height / m	East /°C	Middle /°C	West /°C
10+10 m	1.5	29.63	30.86	29.39
	3.0	30.56	32.23	29.88
	4.5	31.35	32.74	30.47
13+7 m	1.5	30.23	32.16	30.16
	3.0	32.06	32.95	31.32
	4.5	33.08	34.13	32.66
15+5 m	1.5	28.41	28.51	28.31
	3.0	29.06	29.11	29.01
	4.5	30.57	30.62	30.55

It can be seen that the 15+5 m arch shed is the superior one in temperature distribution, but the temperature is lower. The 13+7 m arch shed has advantages in both heat storage capacity and temperature distribution compared with the 10+10 m arch shed. And the temperature distribution of 13+7 m arch shed is acceptable for the consistency of growth of crops. It is concluded that the temperature distribution of asymmetrical arch shed is better than that of symmetrical arch shed within a certain range of the ratio between the sunny side and the shaded side.

Analysis of numerical data

In order to further study the differences of performance between the symmetric and asymmetric arch sheds, numerical simulations are conducted taking the 13+7 m and 10+10 m arch sheds as research objects, which can also provide basic model and method for the further analysis of influence factors. The calculating parameters are set according to the measured data at 14:00 on January 6th.

The temperature and air flow fields in the arch sheds are extracted. Figure 6 shows the comparison of temperature distribution between the two arch sheds along north-south direction. It can be seen that, compared with 10+10 m arch shed, the temperature of 13+7 m arch shed is significantly higher near the crop area because of the larger sunny side span. Besides, the temperature gradient is more obvious in 13+7 m arch shed, which can result in up-down air convection. The two-dimensional velocity vectors are shown in Figure 7. It can be seen that obvious air circulations exist in 13+7 m arch shed and the intensity of the air circulations is greater compared with 10+10 m arch shed. Therefore, the asymmetric arch shed is more conducive to air convection and heat transfer, which is beneficial to growth of crops.

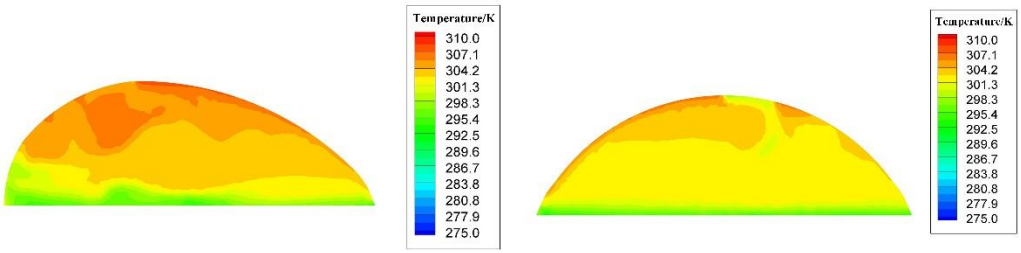

a) 13+7 m *b)* 10+10 m

Fig. 6 - Comparison of north-south temperature distribution

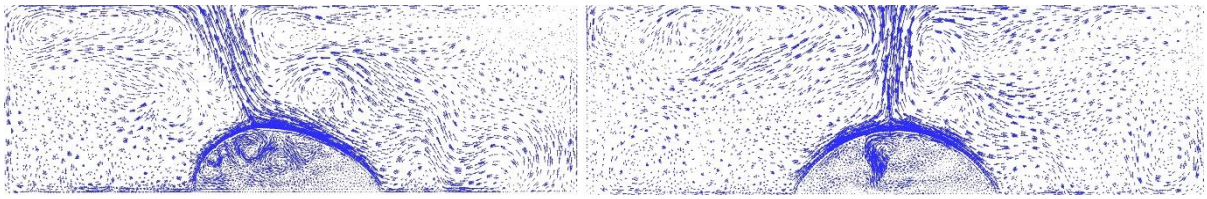

a) 13+7 m *b)* 10+10 m

Fig. 7 - Comparison of north-south velocity vectors

Similarly, Figure 8 shows the comparison of temperature distribution between the two arch sheds along east-west direction.

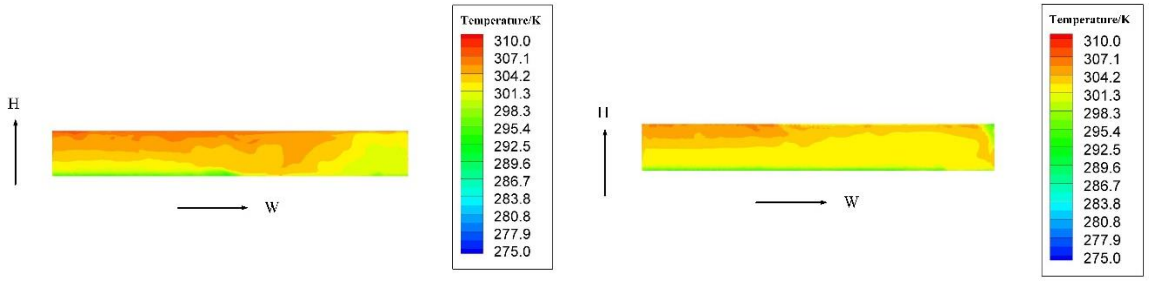

a) 13+7 m *b)* 10+10 m

Fig. 8 - Comparison of east-west temperature distribution

It can be found that the two arch sheds both have a higher temperature distribution in the western part. This is because of the location of the sun and the shading effect.

However, the 13+7 m arch shed has better performance in east-west temperature distribution. The asymmetric structure enhances the solar radiation reception, and the higher-intensity air convection contributes to the heat distribution on a larger scale, which benefits to the consistency of crops' growth. And the numerical results are consistent with measured data.

Reliability verification of numerical results

In order to verify the reliability of the numerical analysis, numerical simulations of the 13+7 m and 15+5 m arch sheds are conducted. The test data was detected at 14:00 on January 6th, the outside wind speed was 0.3 m/s, and the temperature values at each height are averaged. The numerical results and measured data are shown in Table 4. It can be seen that the difference between the measured value and the numerical value is small, and the error is within the acceptable range, which verifies the reliability of the numerical simulation.

Table 4

Comparison of numerical results and measured data

Arch shed structure	Height / m	Measured / °C	Simulation / °C	Error / %
13+7 m	1.5	30.85	29.34	4.89
	3.0	32.11	30.65	4.55
	4.5	33.29	4.69	4.69
15+5 m	1.5	28.41	26.99	5.00
	3.0	29.06	27.54	5.23
	4.5	30.58	28.97	5.26

- **Influences of structure and environmental factors**

In order to further study the influences of arch structural parameters and environmental factors on the temperature field of the arch shed, considering the high cost of test method, the numerical method is adopted to analyse the influence rule and find the optimal range. The parameters of the numerical simulations are set with reference to the measured data at 14:00 on January 6th.

Reliability verification of numerical results

According to the analysis above, it is concluded that the heat storage capacity and temperature distribution of 13+7 m arch shed are better than those of 10+10 m arch shed. Here, in order to further analyse the influence of the span ratio between the sunny and shaded sides, ten different asymmetric arch sheds are designed, which have the sunny side span ranged from 10.5 m to 15 m with an interval of 0.5 m. Figure 9 shows the average temperature curves at the three heights. It can be found that the average temperature curves have similar trends, and the average temperature of asymmetrical arch shed is higher than that of asymmetrical arch shed within a certain range. Especially, the 11+9 m arch shed achieves the highest average temperature. However, with the span of sunny side increases, this advantage of asymmetrical arch shed is not constant and the differences of average temperature become larger at different heights. As it is known, the solar radiation reception mainly depends on solar reception area and solar angle of incidence. The relationship between the film transmittance and the solar angle of incidence is as follows.

$$\tau_t = 90 - 5^{(i_t - 20)/25.06} \quad (1)$$

Where, i_t is the solar incident angle, τ_t is the film transmittance. With the span of sunny side increases, the solar reception area increases, but the solar angle of incidence increases correspondingly, and that is not conducive to the absorption of solar radiation. As discussed previously, the average temperature at 14:00 can represent the heat storage capacity of the arch shed, so it can be considered that the optimal span ratio between the sunny and shaded sides is about 11:9.

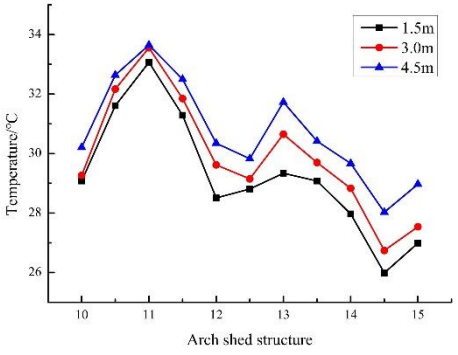

Fig. 9 - Temperature under different structures

Influence of wind speed

In order to ensure the air exchange between inside and outside of arch shed and reduce the temperature in certain situations, the vent will be opened for ventilation. Therefore, the influence of outside wind speed on temperature field in arch shed should be considered. In this paper, the analysis mainly focuses on the low temperature situation, so the top vent is open with 0.3 m and the side vents remain closed in numerical simulations. Taking 13+7 m arch shed as an example, the average temperatures at different heights are shown in Table 5. It can be found that the average temperatures decrease significantly with the outside wind speed increases.

Table 5

Temperature under different outside wind speeds

Velocity/(m/s)	1.5 m Height/℃	3 m Height/℃	4.5 m Height/℃
1.6	20.21	20.77	21.67
3.4	13.11	13.03	13.25
5.5	10.44	10.53	10.60
8.0	9.15	8.48	8.43

Figure 10 shows the comparison of two-dimensional velocity vectors under different outside wind speeds along north-south direction. When the outside wind speed equals 1.6 m/s, the air convection is relatively weak and the velocities mainly exist near the top vent. With the outside wind speed increases, the large-scale air circulations begin to appear and the velocities gradually increase. That is, the air exchange and heat transfer become fiercer. Therefore, when the outside wind speed is high, the opening time of top vent should be shortened or the opening size should be reduced to keep a suitable temperature in arch shed. In order to further verify the accuracy of the numerical results, measured data on January 1th, January 14th and January 20th are chosen to make a comparison, and the wind speed is 1.3 m/s, 2.8 m/s and 4.3 m/s respectively. The difference between measured data and numerical value is small, so the numerical results and analysis are reliable.

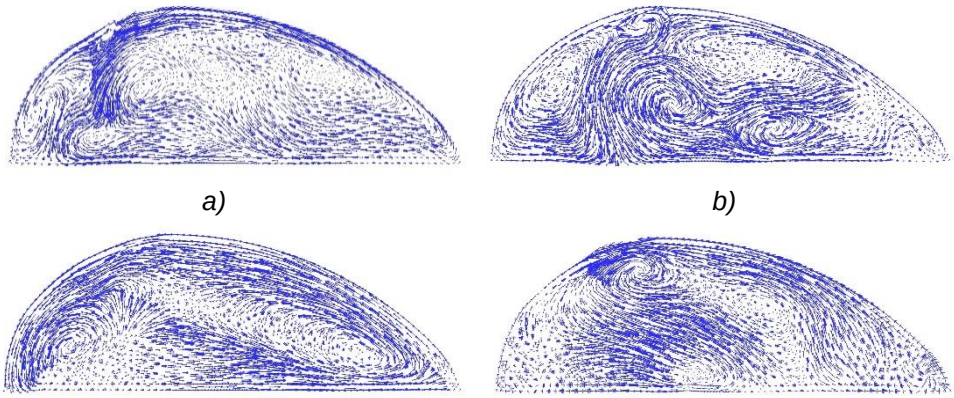

a) *b)* *c)* *d)*

Fig. 10 - Comparison of two-dimensional velocity vectors under different outside wind speeds

a) 1.6 m·s^{-1} ; *b)* 3.4 m·s^{-1}; *c)* 5.5 m·s^{-1} ; *d)* 8.0 m·s^{-1}

Influence of top vent

The air exchange between inside and outside of arch shed is necessary for the growth of crops. Besides, the ventilation is an efficient measure of temperature control. Using 13+7 m arch shed as an example, the opening sizes of top vent are set to 0 m, 0.2 m, 0.3 m, 0.4 m, 0.5 m, 0.6 m, 0.7 m, 0.8 m, 0.9 m and 1.0 m to analyse the influences of top vent to temperature field, and the numerical results are shown in the Figure 11. With the increase of opening size of top vent, there appears a downward trend of average temperature in the arch shed, and the differences among different heights become smaller due to more powerful up-down air exchange and heat transfer. In agricultural production, the opening size of top vent should be determined by weather, wind speed and outside temperature. In order to further verify the accuracy of the numerical results, measured data on January 3th, January 6th and January 7th are chosen to make a comparison, and the opening size of top vent is 0.2 m, 0.3 m and 0.4 m respectively. The difference between measured data and numerical value is small, so the numerical results and analysis are reliable.

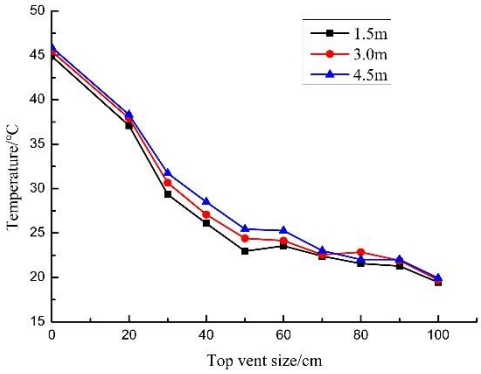

Fig. 11 - Temperature under different opening size of top vent

Comprehensive analysis of factors

The influences of structural parameter, outside wind speed and opening size of top vent have been discussed respectively. Here, the response surface method (RSM) is adopted to establish the mathematical relationship of temperature with structure of arch shed, outside wind speed, and opening size of top vent *(Xiong Shen et al., 2012)*. The influence factors and division levels are shown in Table 6. The average temperature at the height of 1.5 m is taken as target parameter. Figure 12 shows the corresponding surface of any two factors.

Table 6

Division levels of influence factors

Level	Structure of arch shed	Outside wind speed/(m·s^{-1})	Opening size of top vent /cm
-1.732	10.5:9.5	1.1	20
-1	11.0:9.0	1.6	30
0	11.5:8.5	2.1	40
1	12.0:8.0	2.6	50
1.732	12.5:7.5	3.1	60

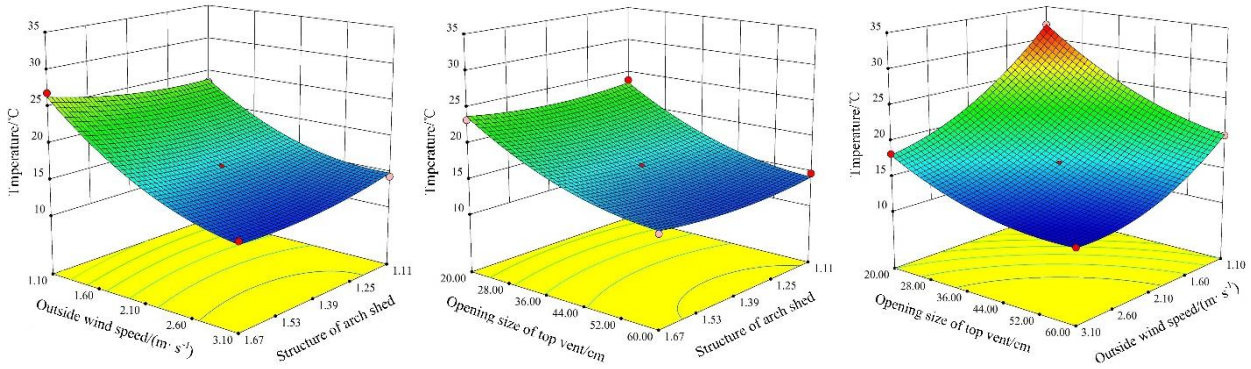

a) *b)* *c)*

Fig. 12 - Corresponding surface of any two factors

Through the statistical analysis of Design-Expert software, it is concluded that the secondary multiple regression equation of temperature with structure, wind speed, and opening size of top vent can be described as follows.

$$Y = 70.92 - 21.91\mathrm{A} - 13.37\mathrm{B} - 0.77\mathrm{C} - 3.99\mathrm{AB} - 0.00464\mathrm{AC} + 0.76\mathrm{BC} + 11.18\mathrm{A}^2 + 2.45\mathrm{B}^2 + 0.00482\mathrm{C}^2 \quad (2)$$

Where, A represents the level of span ratio between the sunny and shaded sides, B represents the level of outside wind speed, C represents the level of opening size of top vent, and Y represents the average temperature in arch shed. As it is shown in the formula, the structure of arch shed, outside wind speed and opening size of top vent can be adjusted for an expected temperature. The mathematical model would provide prediction and guidance for the design and construction of asymmetric arch shed.

The variance analysis of the regression model is shown in Table 7. When the P value is less than 0.0001, the influence factor is significant. It can be found that the influence factors of outside wind speed and opening size of top vent are significant, as well as their quadratic terms. The span ratio between the sunny and shaded sides is not significant. And the predicted value of the model is very close to the actual value, indicating that the mathematical relationship expression is reliable.

Table 7

Variance analysis

Source	Sum of squares	Freedom	Mean squares	F value	P value
Model	483.19	9	53.69	219.18	<0.0001
A	0.22	1	0.22	0.91	0.3713
B	248.59	1	248.59	1014.88	<0.0001
C	171.59	1	171.59	700.52	<0.0001
AB	4.99	1	4.99	20.38	0.0027
AC	0.002704	1	0.002704	0.011	0.9193
BC	9.35	1	9.35	38.15	0.0005
A^2	3.23	1	3.23	13.20	0.0084
B^2	25.27	1	25.27	103.17	<0.0001
C^2	15.65	1	15.65	63.91	<0.0001
Residual	1.71	7	0.24		
Lack of fit	1.71	3	0.57		
Pure error	0.000	4	0.000		
Cor Total	484.90	16			

CONCLUSIONS

In this paper, an east-west large-span arch shed with asymmetric structure was designed. The east-west length of the arch shed is 50 m, the north-south span is 20 m, and the height of the arch shed is 6.5 m. The sunny side has a larger span. The arch shed is equipped with top vent and side vents to realize ventilation. Based on computational fluid dynamics, numerical model of air flow behaviours and heat transfer in the arch shed was established.

According to the measured data, numerical simulations of air flow behaviour and heat transfer process in the arch shed were conducted. It is shown that the thermal environment in arch shed is affected by solar radiation and air convection. Under low outside temperature, compared with the 10+10 m arch shed, the 13+7 m arch shed has increases of temperature by 2.97%, 3.95% and 5.62% at the height of 1.5 m, 3.0 m and 4.5 m respectively. Besides that, the uniformity of east-west temperature distribution of the 13+7 m arch shed is also improved. It can be concluded that both the heat storage capacity and the temperature distribution uniformity of asymmetric arch shed are superior to those of symmetric arch shed within a certain range of the ratio between the sunny side and the shaded side.

The influences of arch shed structure, outside wind speed and opening size of top vent to the temperature in the arch shed under low outside temperature were analysed. The results show that the 11+9 m arch shed has the best heat storage performance. The outside wind and top vent can promote the air exchange between inside and outside, enhance the intensity of inside air convection, and then reduce the temperature in arch shed. Finally, the relationship of temperature with arch shed structure, outside wind speed, and opening size of top vent was built based on response surface methodology.

ACKNOWLEDGEMENT

This work was supported by the China Postdoctoral Science Foundation (2019M662410), the National Key Research and Development Project of China (2017YFD070150) and the National Characteristic Vegetable Industry Technology System Project (CARS-24-D-01).

REFERENCES

[1] Banu J.P., Mani A., (2019), Numerical studies on ejector with swirl generator, *International Journal of Thermal Sciences*, Vol.137, pp.589-600;

[2] Bartzanas T., Boulard T., Kittas, C., (2004), Effect of vent arrangement on windward ventilation of a tunnel greenhouse, *Biosystems Engineering*, Vol.88, Issue 4, pp.479-490;

[3] Changji Zhou, Yingkuan Wang, (2001), Modern greenhouses and their performances in China, *Transactions of the Chinese Society of Agricultural Engineering*, Vol.17, Issue 1, pp.16-21;

[4] Fei Qi, Xinqun Zhou, Yuefeng Zhang, et al., (2008), Development of world greenhouse equipment and technology and some implications to China, *Transactions of the Chinese Society of Agricultural Engineering*, Vol.24, Issue 10, pp.279-285;
[5] Ghenai C., Janajreh I., (2010), CFD analysis of the effects of co-firing biomass with coal, *Energy Conversion and Management*, Vol.51, Issue 8, pp.1694-1701;
[6] Guohong Tong, Christopher, D.M., Guoqiang Zhang, (2017), New insights on span selection for Chinese solar greenhouses using CFD analyses, *Computers and Electronics in Agriculture*, Vol.149, pp.3-15;
[7] Guohui Guo, (2009), CFD modelling of transparent bubble cavity envelopes for energy efficient greenhouses, *Building and Environment*, Vol.44, Issue 12, pp.2486-2500;
[8] Guzmán C., Carrera J., Durán H., et al., (2019), Implementation of virtual sensors for monitoring temperature in greenhouses using CFD and control, *Sensors*, Vol.19, Issue 1;
[9] Kichah A., Bournet P.E., Migeon C., et al., (2012), Measurement and CFD simulation of microclimate characteristics and transpiration of an impatiens pot plant crop in a greenhouse, *Biosystems Engineering*, Vol.112, Issue 1, pp.22-34;
[10] Kim K., Yoon J.Y., Kwon, H.J., et al., (2008), 3-D CFD analysis of relative humidity distribution in greenhouse with a fog cooling system and refrigerative dehumidifiers, *Biosystems Engineering*, Vol.100, Issue 2, pp.245-255;
[11] Kruggel-Emden H., Rickelt S., Stepanek F., et al., (2010), Development and testing of an interconnected multiphase CFD-model for chemical looping combustion, *Chemical Engineering Science*, Vol.65, Issue 16, pp.4732-4745;
[12] López-Martinez J., Blanco-Claraco J.L., Perez-Alonso J., et al., (2018), Distributed network for measuring climatic parameters in heterogeneous environments: Application in a greenhouse, *Computers and Electronics in Agriculture*, Vol.145, pp.105-121;
[13] Majdoubi H., Boulard T., Fatnassi H., et al., (2009), Airflow and microclimate patterns in a one-hectare canary type greenhouse: an experimental and CFD assisted study, *Agricultural and Forest Meteorology*, Vol.149, Issue (6-7), 1050-1062;
[14] Mobtaker H.G., Ajabshirchi, Y., Ranjbar, S.F., et al., (2016), Solar energy conservation in greenhouse: thermal analysis and experimental validation, *Renewable Energy*, Vol.96, Issue 1, pp.509-519;
[15] Perén J.I., Hooff T., Leite, B.B., et al., (2015), CFD analysis of cross-ventilation of a generic isolated building with asymmetric opening positions: Impact of roof angle and opening location, *Building and Environment*, Vol.85, pp.263-276;
[16] Piscia D., Montero J.I., Baeza E., et al., (2012), A CFD greenhouse night-time condensation model, *Biosystems Engineering*, Vol.111, Issue 2, pp.141-154;
[17] Saberian A., Sajadiye S.M., (2019), The effect of dynamic solar heat load on the greenhouse microclimate using CFD simulation, *Renewable Energy*, Vol.138, pp.722-737;
[18] Singh R.I., Brink A., Hupa, M., (2013), CFD modelling to study fluidized bed combustion and gasification, *Applied Thermal Engineering*, Vol.52, Issue 2, pp.585-614;
[19] Xiangli He, Jian Wang, Shirong Guo, et al., (2017), Ventilation optimization of solar greenhouse with removable back walls based on CFD, *Computers and Electronics in Agriculture*, Vol.149, pp.16-25;
[20] Xiong Shen, Guoqiang Zhang, Bjerg B., (2012), Investigation of response surface methodology for modelling ventilation rate of a naturally ventilated building, *Building and Environment*, Vol.54, pp.174-185.